SWIFT-XRT-CALDB-09

Release Date: May 31st, 2010

Prepared by: Andrew Beardmore[1], Olivier Godet[1,2], Claudio Pagani[1], Sergio Campana[3]

Date revised: May 26th, 2010

Revision: 14

Revised by: Andrew Beardmore

[1] Leicester, [2] CESR, [3] INAF-OAB

SWIFT XRT CALDB RELEASE NOTE SWIFT-XRT-CALDB-09: Response matrices and Ancillary Response Files

Table 1: Files to be released:

Filename	Mode	Grade	Substrate* voltage (V)	Start time°	End time°	Release Date
swxwt0to2s6_20070901v012.rmf †	WT	0-2	6	31-Aug-2007		31-May-2010
swxwt0to2s6_20010101v012.arf ‡	WT	0-2	6	31-Aug-2007		31-May-2010
swxwt0s6_20070901v012.rmf †	WT	0	6	31-Aug-2007		31-May-2010
swxwt0s6_20010101v012.arf ‡	WT	0	6	31-Aug-2007		31-May-2010

*The substrate voltage was permanently raised from $V_{ss} = 0\,\mathrm{V}$ to $V_{ss} = 6\,\mathrm{V}$ on 2007 August 30 (see below).

° Start and end validity time when the RMFs should be used.

† New $V_{ss} = 6\,\mathrm{V}$ WT RMFs

‡ New $V_{ss} = 6\,\mathrm{V}$ WT ARFs

Scope of Document

This note describes the release of updated *Swift*-XRT Windowed Timing (WT) redistribution matrix files (RMFs) and auxillary response files (ARFs), appropriate for substrate voltage $V_{ss} = 6\,\mathrm{V}$ data (RMF v012) taken since 2007-Aug-31 (see Table 1).

Preamble

The XRT effective area is made up of three main components: the mirror effective area, the CCD quantum efficiency (QE) and the filter transmission. The QE is included directly in the redistribution matrix files (RMFs). The auxillary response files (ARFs) contain the mirror effective area, the filter transmission, as well as the vignetting correction and the Point Spread Function (PSF) correction, which depends on the source location and of the size of the extraction region, as well as on defects on the CCD (such as 'bad columns' or 'hot pixels', which are flagged as unsuitable for data analysis).

Here we report on the CALDB RMF and ARF files, the latter representing the effective area of the telescope for a nominal on-axis observation (no vignetting correction) and for an infinite region of interest (no correction for PSF losses). RMF files do not include the PSF correction and do not depend on the source position on the detector. The CCD low energy spectral response is sufficiently uniform within the central 200x200 pixels (see, for example, previous RMF release notes), therefore there is just one RMF file per mode and grade selection and per epoch. The ARF file for any given observation, instead, needs vignetting and PSF corrections and, therefore, needs to be built for each observation. To produce the observation-specific ARF files, the XRTMKARF task (part of the XRTDAS-HEADAS software) is used. This task corrects the nominal ARF file from the CALDB for the vignetting and, optionally (*psfflag=yes*), for PSF losses. This task includes corrections for CCD defects with the inclusion of an exposure map which can be automatically generated by the data analysis pipeline (*expofile=filename.img*).

Motivation behind this release

The XRT suffered a thermoelectric cooler power supply failure shortly after launch which meant the CCD could not be operated at the expected nominal temperature of $-100\,^{\circ}\mathrm{C}$. However, by carefully controlling the spacecraft pointing during pre-planned science observations the CCD can be passively cooled to acceptable temperatures in the range ~ -75 to $-50\,^{\circ}\mathrm{C}$ (Kennea et al. 2005, SPIE, 5898, 329).

Furthermore, laboratory testing showed that by raising the CCD substrate voltage from $V_{ss} = 0\,\mathrm{V}$ to $V_{ss} = 6\,\mathrm{V}$ the thermally induced dark current in the CCD could be reduced, allowing the CCD to operate a few degrees warmer before excessive hot pixels compromise data (Godet et al., 2009, A&A, 494, 775). Because of this, the XRT CCD substrate voltage was permanently raised to $V_{ss} = 6\,\mathrm{V}$ on 2007 August 30 (at 14:28UT).

A consequence of changing the substrate voltage is that the CCD depletion depth has decreased slightly which, in turn, has altered the QE at high energies and just below the Si edge ($\sim 1.5 - 1.84\,\mathrm{keV}$). The latter, in particular, has been noticeable when spectra of sufficient signal-to-noise from observations taken since the substrate voltage change are analysed with the previously released RMFs/ARFs (for example, see figure 1(a)).

In this release, the WT RMFs and ARFs are newly computed files appropriate for $V_{ss} = 6\,\mathrm{V}$ observations — i.e. those taken since 2007 August 30.

RMF/ARF file naming scheme

The change in substrate voltage made it necessary to release two sets of RMF/ARF files, distinguished by the characters 's0' and 's6' in their filenames. The filenames also encode the XRT readout mode (WT in this case), the grade selection ($0-2$ or 0) and the epoch the files should be used from (after epoch dependent broadening has been applied). The files released this time are, for WT grade $0-2$:

swxwt0to2s6_20070901v012.rmf
swxwt0to2s6_20010101v012.arf

and for WT grade 0 :

swxwt0s6_20070901v012.rmf
swxwt0s6_20010101v012.arf

RMF generation

The Response Matrix Files (RMFs) are created by a Monte-Carlo simulation code (Godet et al. 2009, A&A, 494, 775, and references therein). This code models: transmission of the incident X-rays through the CCD electrode structure; photo-absorption in the active layers of the device (i.e. the depletion and field-free regions); charge cloud generation, transportation and spreading; silicon fluorescence and its associated escape peak; surface loss effects; mapping of the resultant charge-cloud to the detector pixel array; charge transfer efficiency; addition of electronic read-out noise; event thresholding and classification according to the specific mode of operation.

Improvements specific to this release

For this release, WT RMFs have been created in which the CCD depletion depth (DD) has been modified to be more appropriate for $V_{ss} = 6\,\mathrm{V}$ operation. To find the most appropriate DD, WT RMFs were computed with different DDs ranging from 18–30 microns. Then, using an unmodified ARF file based on the ray-traced mirror area file, but including a correction to the gold edge depth (as has been required previously), the RMFs were tested on a Cyg X-1 dataset, which was observed simultaneously with Suzaku (XIS0 and XIS1) on 2009-May-06. A DD 22 micron RMF was found to agree with the Suzaku derived spectral parameters above 2 keV (c.f. the DD 27 micron RMF for $V_{ss} = 0\,\mathrm{V}$ observations).

After applying the same level of broadening to the RMF appropriate for the 2007-Sep epoch (as described in the release note SWIFT-XRT-CALDB-09_v12), high signal-to-noise observations of Mkn 421 were used to provide further corrections to the RMF QE around the silicon edge and the ARF gold M-shell edge regions. Figure 1(a) shows the improvements obtained when fitting the Mkn 421 data with the new v012 RMF/ARF.

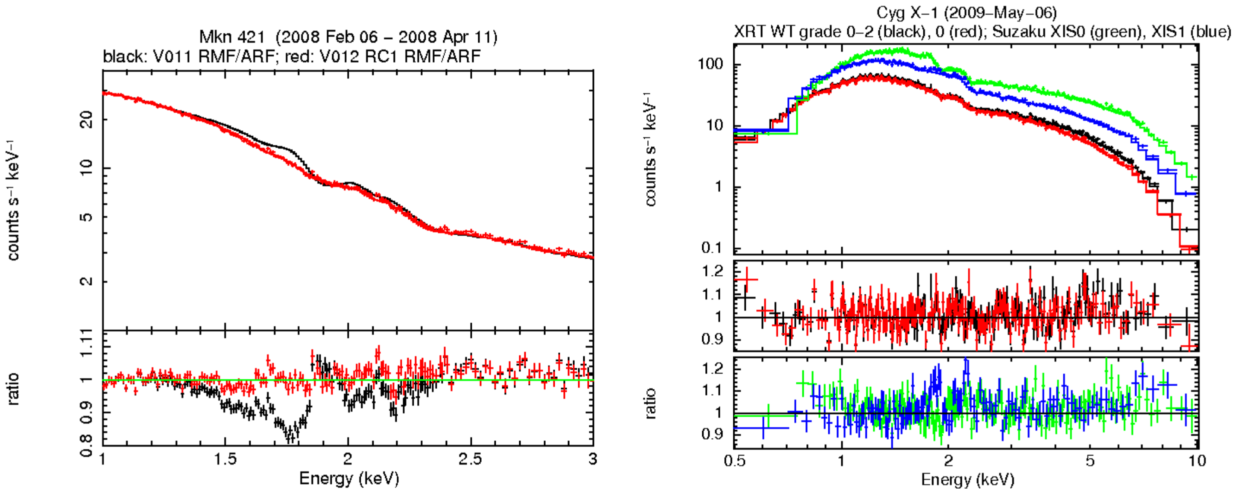

Figure 1: Left (a): Mkn 421 XRT WT grade $0-2$ spectrum from observations taken 2008-Feb-06 to 2008-Apr-11, fit with the v011 RMF/ARF (black) and the new v012 RMF/ARF (red). The $\sim 15\%$ residuals seen around 1.8 keV in the v011 fit are reduced to less than 3% in the v012 fit. Right (b): XRT WT (grade $0-2$ in black, grade 0 in red, fit with the new v012 RMF/ARF) and Suzaku XIS0 (green), XIS1 (blue) spectra from a simultaneous observation of Cyg X-1 on 2009-May-06.

Some results of tests on the RMF/ARFs are given below. Table 2 compares the parameters obtained when fitting the XRT and Suzaku XIS0/1 spectra from Cyg X-1, showing good agreement between the instruments (see figure 1(b)). Likewise, table 3 shows a comparison of the spectral fit results obtained for the blazar PKS2155–304 from data taken simulataneously with XMM MOS1/MOS2/PN on 2009-May-28.

Table 2: XRT WT and Suzaku XIS0/1 spectral fit results from a simultaneous observation of Cyg X-1 obtained on 2009-May-06. Model: PHABS * (DISKBB + POWERLAW).

Instrument	XIS0/1	XRT WT	
		grade $0-2$	grade 0
NH[a]	0.857 ± 0.054	0.902 ± 0.053	0.862 ± 0.054
diskbb kT[b]	0.223 ± 0.017	0.210 ± 0.016	0.220 ± 0.020
diskbb norm[c]	$2.05^{+1.58}_{-0.92}$	$2.48^{+1.9}_{-1.1}$	$1.58^{+1.45}_{-0.77}$
photon index, Γ	1.795 ± 0.028	1.786 ± 0.030	1.792 ± 0.033
F_x[d]	$11.08^{+0.07}_{-0.22}$ (XIS0) $10.55^{+0.07}_{-0.22}$ (XIS1)	$9.38^{+0.06}_{-0.16}$	$9.25^{+0.08}_{-0.22}$

[a] Column density ($\times 10^{22}\mathrm{cm}^{-2}$); [b] Disc blackbody temperature (keV); [c] Disc blackbody normalisation ($\times 10^5$); [d] $0.5-10\,\mathrm{keV}$ flux ($\times 10^{-9}\,\mathrm{erg\,cm^{-2}\,s^{-1}}$)

Spectra of the soft neutron star source RXJ1856.4–3754 taken in 2007 November, 2008 March, 2008 September and 2009 October, fit with the model described in Beuermann et al. (2006, A&A, 458, 541) using the v012 response files, reveal a relative normalisation within 6 per cent for the 4 epochs.

Figure 2 shows the estimated WT QE and total effective area for both the grade 0–2 and grade 0 for the v012 RMF/ARFs.

Table 3: XRT WT and XMM MOS1/MOS2/PN spectral comparison for a simultaneous observation of PKS2155−304 taken on 2009-May-28. Model : PHABS * BKNPOW with NH fixed at the galactic value of $1.48 \times 10^{20}\,\mathrm{cm}^{-2}$.

	MOS1	MOS2	PN	XRT WT	
				grade 0 − 2	grade 0
$\Gamma_1{}^a$	$2.643^{+0.025}_{-0.026}$	$2.593^{+0.027}_{-0.041}$	2.707 ± 0.012	$2.502^{+0.026}_{-0.028}$	$2.499^{+0.026}_{-0.028}$
$E_b{}^b$	$1.316^{+0.137}_{-0.170}$	$1.261^{+0.103}_{-0.193}$	1.059 ± 0.065	$1.249^{+0.096}_{-0.107}$	$1.243^{+0.097}_{-0.114}$
$\Gamma_2{}^c$	$2.852^{+0.049}_{-0.042}$	$2.945^{+0.049}_{-0.059}$	2.885 ± 0.016	$2.896^{+0.046}_{-0.044}$	$2.891^{+0.049}_{-0.047}$
$F_x{}^d$	$1.21^{+0.02}_{-0.01}$	$1.22^{+0.01}_{-0.02}$	1.27 ± 0.01	1.26 ± 0.01	1.27 ± 0.01

[a] photon index below the break; [b] break energy; [c] photon index above the break;
[d] $0.3 - 10\,\mathrm{keV}$ flux ($\times 10^{-10}\,\mathrm{erg\,cm^{-2}\,s^{-1}}$)

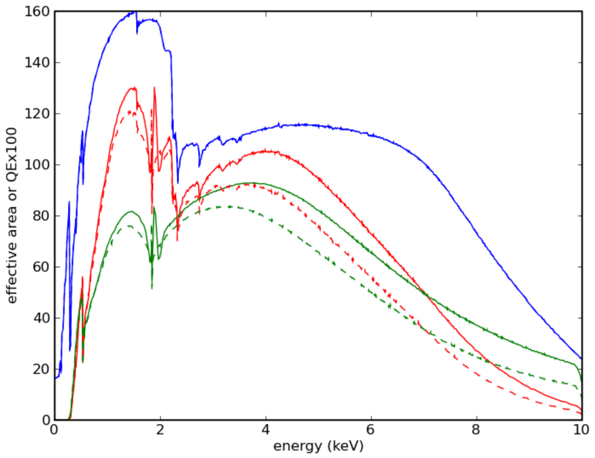

Figure 2: The WT v012 on axis ARF file is shown in blue, together with the WT grade 0 − 2 QE in solid green and the total area (ARF*QE) in solid red. The corresponding grade 0 curves are shown dashed.

Current limitations and future prospects

The following considerations apply to WT spectra fit with the RMFs/ARFs described here:

- We have discovered a WT redistribution problem for spectra from heavily absorbed sources with a column density in excess of a $\sim 10^{22}\,\mathrm{cm}^{-2}$. The problem manifests itself as a 'bump' at low energies (typically below 1 keV) in the grade 0–2 spectrum from such sources, with a 'turn-up' at the low energy end (below ~ 0.4 keV). The bump is a consequence of heavy redistribution occuring in grade 1 and 2 events which are then cut off quickly by the onboard event threshold. Grade 0 events do not show the bump, though the turn-up is still present. If a heavily absorbed source has been observed in WT mode we recommend comparing both its grade 0 and grade 0–2 spectra and if differences below ~ 1 keV are apparent to use the grade 0 spectrum for further analysis.

- Over time, the accumulated radiation dose and high-energy proton interactions cause damage to the CCD (in the imaging area, the store frame area and the serial register) resulting in a build-up of charge traps (i.e. faults in the Si crystalline structure of the CCD which hold onto some of the charge released during an X-ray interaction). The deepest traps are responsible for the line FWHM degradation, with the line shape then showing a more pronounced low energy wing. The most serious of these charge traps can cause a loss of up to ~ 600 eV at 6 keV and ~ 300 eV at 1.856 keV from the incident X-ray energy.

  While we released a set of broadened WT RMFs to account for the average line broadening behaviour up to 2008 (see the release note SWIFT-XRT-CALDB-09_v12), and planned a further epoch dependent release, the build up of deep traps in certain CCD columns has meant we can no longer find a generic RMF broadening function which works well for different locations on the detector. This means the current v012 RMF redistribution kernel, which is broadened for the 2007-Sep epoch, is too narrow for datasets taken in 2009 (and later), resulting in measured line widths broader than expected.

- A further consequence of the build up of traps is that, depending on the location of the source on the detector, powerlaw-like spectra can occasionally show 10% residuals around the oxygen edge (near 0.545 keV), caused by a mis-match in the observered and expected energy scales. Such residuals can be improved through careful use of the *gain fit* command in XSPEC by allowing the gain offset to vary by $\sim \pm 20$ eV.

- The traps can also cause spectral residuals for relatively unabsorbed sources at low energies, whereby the data/model ratio turns up (or down) quickly below ~ 0.35 keV. If spectra are believed to be affected then this region of the spectrum should be ignored when fitting.

- Prospects to implement a column by column description of the bias correction in the ground software enabling to correct for the effects of traps are under investigation for PC and WT data after June 2007 (see Fig.4 in the release SWIFT-XRT-CALDB-09_v11 and Godet et al. 2009, A&A, 494, 775).

- The RMF/ARF released here only addresses WT mode. High statistical quality PC mode data can also show Si edge residuals similar to those shown in black in figure 1(a), although in practise this is a rarer occurrence due to the lower count rates of PC mode targets. A PC mode RMF more suited for $V_{ss} = 6\,\mathrm{V}$ operation will be released in due course.

Useful Links

Summary of XRT RMF/ARF releases	http://www.swift.ac.uk/Gain_RMF_releases.html
XRT analysis at GSFC	http://swift.gsfc.nasa.gov/docs/swift/analysis
XRT analysis threads at Leicester	http://www.swift.ac.uk/XRT.shtml
XRT digest pages at Leicester	http://www.swift.ac.uk/xrtdigest.shtml